# Low-temperature surface treatments of CdHgTe using the PE-ALD method before $HfO_2$ deposition*

© I.A. Krasnova, E.R. Zakirov, G.Yu. Sidorov, I.V. Sabinina

Rzhanov Institute of Semiconductor Physics, Siberian Branch, Russian Academy of Sciences,
630090 Novosibirsk, Russia

E-mail: krasnovaia@isp.nsc.ru

*Received April 19, 2024*
*Revised May 14, 2024*
*Accepted May 14, 2024*

The development of methods for surface passivation of narrow-gap semiconductors, in particular CdHgTe, is an actual problem nowadays. One of the promising protective and passivating insulators is hafnium oxide. In this work, the effects of different methods of CdHgTe surface treatment, performed in a plasma-enhanced atomic layer deposition (PE-ALD) system immediately prior to the deposition of $HfO_2$ thin films, on the electrophysical characteristics of the resulting insulator–semiconductor interface are investigated. The values of the built-in charge density and slow trap states have been calculated, and the change of donor concentration in the near-surface region of the semiconductor has been estimated. The chemical composition of the formed intermediate layers was examined.

**Keywords:** CdHgTe, mercury cadmium telluride, MCT, surface passivation, atomic layer deposition, $HfO_2$, MIS structures, C−V characteristics, XPS.

DOI: 10.61011/SC.2024.03.58835.6337H

## 1. Introduction

Cadmium–mercury–tellurium ($Cd_xHg_{1-x}Te$) is a well-known narrow-band semiconductor used for manufacturing of infrared optoelectronic devices [1–4], as well as for the development of lasers and THz radiation detectors [5,6], for studying topological insulators and two-dimensional electron gas [7].

Passivation and protection of the semiconductor surface is one of the important stages of the creation of semiconductor devices, including CdHgTe-based devices, which includes not only the application of a dielectric coating, but also its pretreatment. The key requirements for passivation of the semiconductor surface include ensuring low densities of surface states and effective fixed charge. The use of various dielectrics and wide-band semiconductors for CdHgTe passivation is widely described in the literature, the most common of which are ZnS [8,9] and CdTe [10,11]. Recent studies have shown that dielectric films of $HfO_2$ obtained by plasma–enhanced atomic layer deposition (PE-ALD) at 120°C are also a promising passivating coating for CdHgTe [12]. However, well-known studies of CdHgTe passivation practically do not pay any attention to the state of its surface before dielectric deposition. We have previously shown that it has a significant effect on the electrophysical characteristics of the dielectric–CdHgTe interface [13].

The impact of several methods of preparation of the CdHgTe surface before application of a dielectric coating of $HfO_2$ on the electrophysical parameters of the formed interface is studied in this paper.

* XXVIII International Symposium „Nanophysics and Nanoelectronics“, Nizhny Novgorod, 11−15 March 2024

## 2. Experiment procedure

The studies were carried out on $Cd_{0.22}Hg_{0.78}Te$ grown by molecular beam epitaxy on a Si(013) substrate using ZnTe and CdTe buffer layers. The undoped epitaxial CdHgTe film had an electronic type of conductivity with an electron concentration determined by the contactless Hall method, $\sim 5 \cdot 10^{14}\,cm^{-3}$. The wafer was divided into many samples, which were subjected to various treatments, after which $HfO_2$ was deposited on them and metal–dielectric–semiconductor (MDS) structures were fabricated.

A sample on which $HfO_2$ was applied without pretreatment was accepted as a reference. The remaining CdHgTe samples were chemically cleaned from native oxide and surface contaminants using aqueous ammonia ($NH_4OH$) [14]. Two types of samples were obtained by oxidation in a remote RF discharge plasma generated in an atomic layer deposition system (pressure of $O_2$ — 15 mTorr; RF generator power — 300 W), for 1 and 10 min at room temperature. Another method of preparation consisted in atomic layer deposition of an ultra-thin AlN layer using a trimethylaluminium (TMA) precursor and a remote RF discharge plasma in a nitrogen atmosphere (ultra-high purity). 30 deposition cycles were performed at a substrate temperature of 100°C. Another type of structures was fabricated similarly but using a mixture of gases $O_2$ and $N_2$ (1 : 1) to ignite an RF discharge. Both oxidation and deposition of additional layers using TMA were performed immediately before deposition of the dielectric without exposing the samples to the laboratory atmosphere.

Dielectric films of $HfO_2$ with a thickness of $\sim 20$ nm were applied to CdHgTe samples using the PE-ALD method at a substrate temperature of 120°C.

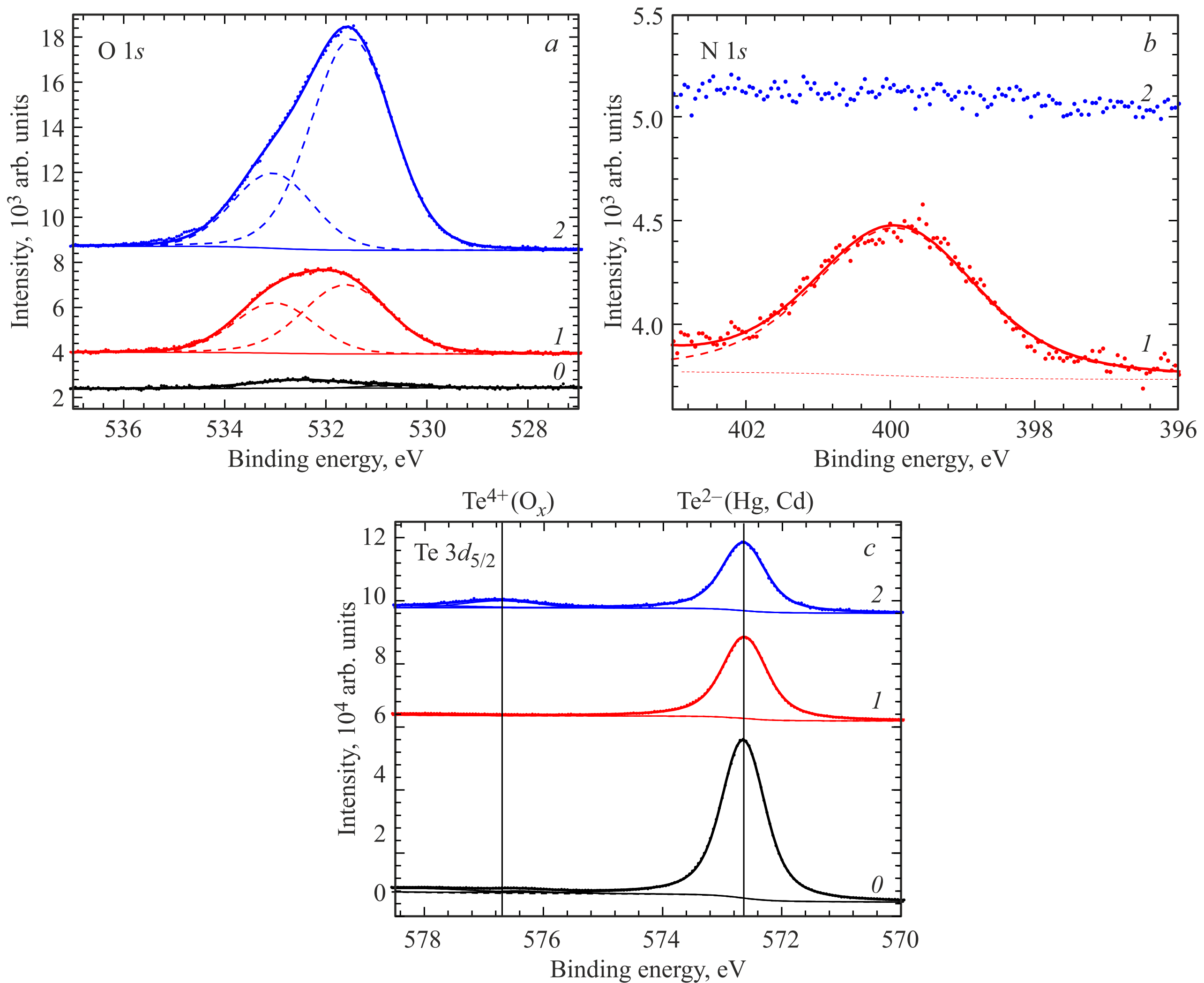


**Figure 1.** Photoelectron lines of O 1$s$ ($a$), N 1$s$ ($b$) and Te $3d_{5/2}$ ($c$) from CdHgTe samples: cleaned in $NH_4OH$ ($0$), with a thin layer of AlN ($1$) and $Al_2O_x$ ($2$) on the surface. The experimental data are shown by dots, and the result of decomposition into components are shown by lines. (A color version of the figure is provided in the online version of the paper).

Tetrakis(ethylmethylamine)-hafnium (TEMAH) was used as a precursor, and remote oxygen plasma of the RF discharge was used as an oxidizer [12]. Round indium contacts with an area of $1.26 \cdot 10^{-3}$ cm$^2$, acting as a metal gate, as well as an ohmic contact to the CdHgTe film were formed using photolithography and thermal evaporation in vacuum.

The coatings obtained on the surface of the CdHgTe as a result of the performed treatments were studied by X-ray photoelectron spectroscopy (XPS) with ProvenX-ARPES system using hemispherical energy analyzer ASTRAIOS 190 2D-CMOS and monochromatized exciting radiation of Al$K_\alpha$. The thickness of the films on the surface of the CdHgTe was evaluated using the method described in Ref. [15].

The frequency dependences of the admittance of the obtained MIS structures were measured at the temperature of liquid nitrogen in the dark using Agilent B1500A semiconductor analyzer. The flat-band voltage ($U_{fb}$), the density of the built-in charge ($N_{fix}$), and the density of slow trap states ($N_t$) for all studied structures were determined from the capacitance–voltage (C–V) curves. The technique described in Ref. [16] was used to determine $U_{fb}$.

## 3. Results

Figure 1 shows the photoelectron lines of O 1$s$, N 1$s$ and Te $3d_{5/2}$ of samples that, after chemical purification, were processed in the PE-ALD system using TMA and remote plasma: nitric and in a mixture of nitrogen and oxygen. It follows from the spectra that the use of a mixture of gases does not result in the formation of aluminum nitride: the position of the line of Al 2$p$ (74.8 eV; not shown in the figure) and the high intensity of the signal of O 1$s$ indicate the formation of aluminum oxide ($Al_2O_x$). Nevertheless, the

presence of nitrogen in the oxide in concentrations below the detection limit of the XPS method is not excluded. On the contrary, the oxygen is present in the film in case of usage of pure nitrogen plasma, and the film itself has a much smaller thickness with the same number of deposition cycles. The presence of oxygen may be a consequence of the oxidation of AlN during the transfer of the sample from the PE-ALD system to the XPS system [17] and/or the presence of water vapor and oxygen in the nitrogen atmosphere at the impurity level (both in the gas itself and in the residual atmospere of the vacuum chamber [18]). The thickness of the layers of $Al_2O_x$ and AlN calculated from the intencity reduce of the tellurium photoelectron line is about 4 and 2 nm, respectively, which is consistent with the available data on the deposition rate of $Al_2O_3$ for the system used ($\sim 0.14$ nm per cycle) and concepts of the AlN deposition rate under similar conditions ($\sim 0.05$ nm per cycle [17]).

The photoelectron line of O 1$s$ of AlN and $Al_2O_x$ films (Figure 1, $a$) can be represented by the sum of two components with binding energies of 531.5 and 533.0 eV. The first corresponds to the chemical bonds of Al−O, and the second, as a rule, is associated with hydroxyl groups (Al−OH) [19]. The proportion of Al−OH bonds in the formed $Al_2O_x$ film reaches 25%. In addition, it is noted that the presence of oxygen in the removed plasma results in the formation of tellurium oxide on the surface of the CdHgTe (Figure 1, $c$). The estimate of the average thickness of the CdHgTe oxide from the ratio between $Te^{4+}$ and $Te^0$ components of the Te 3$d$ line corresponds to approximately one monolayer. The oxidation of CdHgTe can occur at the earliest stages of atomic layer deposition, while there is no continuous surface coating, after which the $Al_2O_x$ film acts as a barrier to oxygen radicals.

Without introducing an organometallic precursor into the PE-ALD reactor, the remote oxygen plasma can be used for low-temperature oxidation of cadmium-mercury telluride before dielectric deposition. We have previously shown that this approach allows for a significant reduction of the density of built-in charge and slow surface states in structures with PE-ALD $Al_2O_3$ on CdHgTe [13,20]. Chemically cleaned samples were oxidized in this study for 1 and 10 minutes, as a result of which the native oxide thickness, determined by the XPS method, reached about 1 and 2 nm, respectively.

Figure 2 shows the characteristic low-frequency capacitance–voltage (C−V) dependencies of the MIS structures with different treatment of the CdHgTe surface. The measurements were performed at a frequency of 10 kHz and cyclic sweep of the gate voltage in the forward (from 0.5 to −6 V) and reverse (from −6 to 0.5 V) directions. The studied structures exhibit pronounced C−V curve hysteresis, which develops in proportion to the sweep range [21]. The hysteresis phenomenon is caused by the recharge of slow trap states localized near the dielectric–semiconductor interface. The forward and reverse loops have different steepness and minimum depth, which indicates the heterogeneity of the trap parameters (carrier capture cross-section concentration) according to their energy location and distance from the semiconductor surface. The slow traps are in an equilibrium state at the initial moment of measurements (accumulation mode) and practically do not manifest themselves during the forward sweep. They gradually change their charge in the strong inversion mode in accordance with their position relative to the Fermi level, which results in a change of the effective surface charge and a shift of the C−V curve to the negative bias region. During the reverse course, the traps partially manage to change their charge — a stretching of the C−V curve along the voltage axis is observed. Some of the traps, being in this state, apparently also recharge at the frequency of the measuring signal used, contributing to the measured capacity of the MIS structure (fast traps).

The width of the hysteresis loop at the level of flat-band capacitance given per unit of the sweep range, was used to estimate the density of slow trap states:

$$N_t = \frac{C_{inv}}{qS} \frac{(U_{fb1} - U_{fb2})}{\Delta U_{sweep}},$$

where $C_{inv}$ — maximum capacitance of the structure in the strong inversion mode, $q$ — electron charge, $S$ — metal contact area, $\Delta U_{sweep}$ — voltage sweep range, $U_{fb1}$ and $U_{fb2}$ — flat-band voltages corresponding to the forward and reverse sweep of the C−V curve. The lowest density was achieved in the structure with $Al_2O_x$ and is $1 \cdot 10^{11}\,cm^{-2} \cdot V^{-1}$; the highest density was achieved in the structure with 2 nm of native oxide — $9.6 \cdot 10^{11}\,cm^{-2} \cdot V^{-1}$; the density of the reference sample was $3.0 \cdot 10^{11}\,cm^{-2} \cdot V^{-1}$.

It follows from the obtained data that the preliminary oxidation of CdHgTe in the remote plasma results in a significant increase of the density of traps near the interface of $HfO_2$−CdHgTe compared with cases when the surface of the CdHgTe was chemically cleaned or no treatment was performed at all. Previously, the opposite result was obtained on the CdHgTe in structures with PE-ALD $Al_2O_3$. Such a disagreement can be explained by a significant difference in the physico-chemical processes occurring at the interface between the deposited dielectric and native oxide of CdHgTe, and this interface further has a decisive effect on the hysteresis of the C−V curve of the metal–dielectric–semiconductor structures.

The density of the effective built-in charge was calculated using the formula

$$N_{fix} = \frac{C_{inv}}{qS} (\varphi_{ms} - U_{fb1}),$$

where $\varphi_{ms}$ — the metal-semiconductor work function difference. The calculation results are presented in the table. It follows from these results that structures made on CdHgTe oxidized in a remote plasma are characterized by a positive built-in charge, the value of which increases with the increase of the thickness of the native oxide. At the same time, the remaining structures have a negative built-in charge. It is assumed based on this that the dielectric $HfO_2$

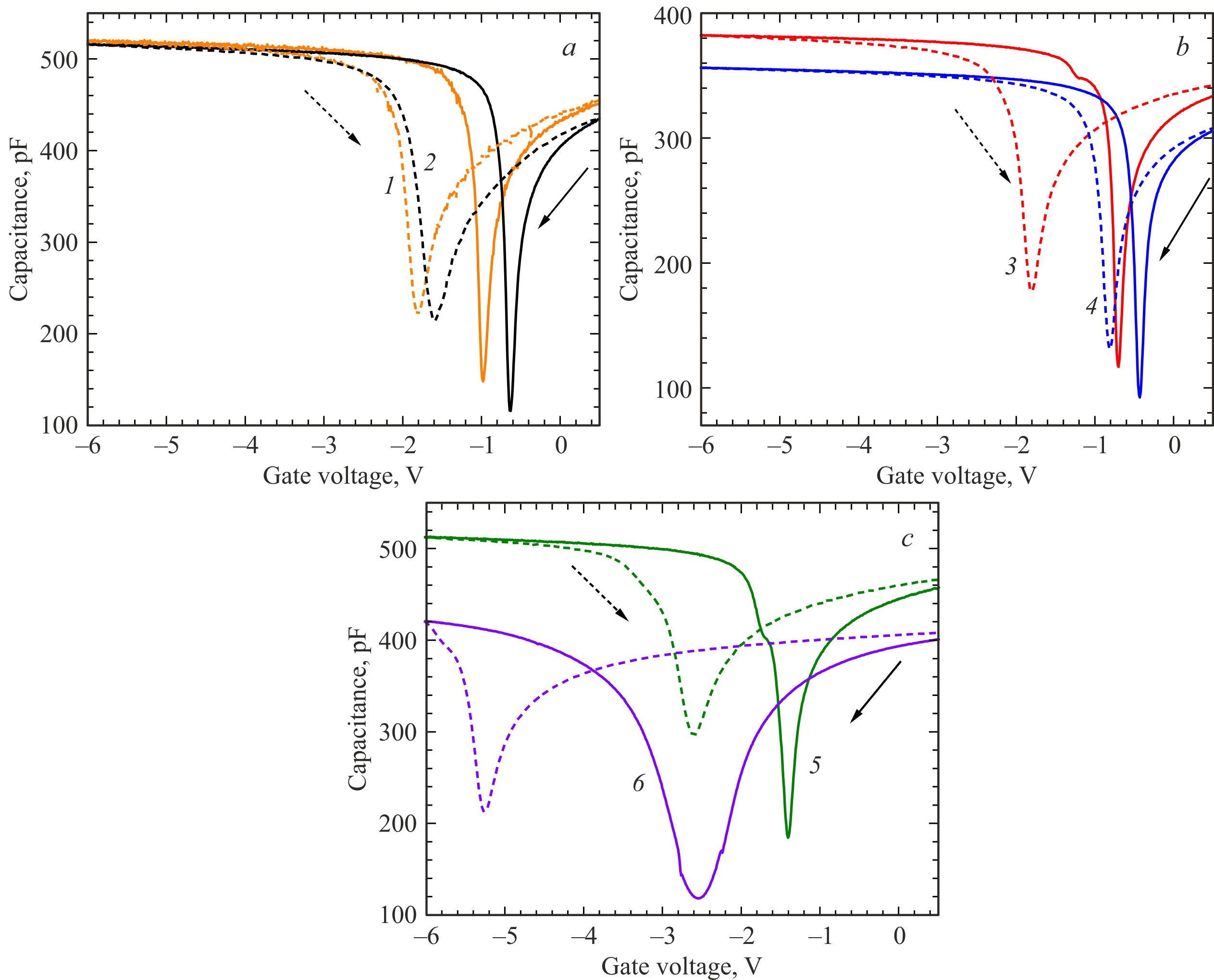


**Figure 2.** The capacitance–voltage curves of MIS structures with various surface treatments of CdHgTe before application $HfO_2$: without additional treatments (*1*); wet cleaning in $NH_4OH$ (*2*); deposition of thin films of AlN (*3*) or $Al_2O_x$ (*4*); oxidation in the remote plasma for 1 (*5*) and 10 min (*6*). The solid line shows the forward direction of the bias sweep, the dotted line shows the reverse direction.

has a volumetric negative charge with an effective density of $\sim 1 \cdot 10^{12}\,\mathrm{cm}^{-2}$, and CdHgTe native oxide formed in oxygen plasma can be used to compensate and minimize it.

The capacitance of structures determined from experimental C–V curves at the voltage of flat bands was used to estimate the concentration of donors ($N_D$) using a known ratio:

$$C_{fb} = \frac{\varepsilon_0 \varepsilon_{ins} S}{d_{ins} + (\varepsilon_{ins}/\varepsilon_s)\sqrt{kT\varepsilon_s\varepsilon_0/N_D q^2}},$$

where $\varepsilon_0$ — dielectric constant of vacuum, $\varepsilon_{ins}$ and $\varepsilon_s$ — dielectric permittivity of dielectric and semiconductor, respectively, $d_{\mathrm{ins}}$ — dielectric thickness, $k$ — Boltzmann constant [22]. The values obtained (see table) exceed the data obtained after epitaxial growth of CdHgTe, which indicates an interruption of the structure of the near-surface region of the semiconductor and the generation of electrically active defects acting as donors. The oxidation of CdHgTe in plasma results in a significant increase of the concentration of donors in the area of the spatial charge of the MIS structures. The lowest concentration of donors was achieved in a structure with an intermediate layer of $Al_2O_x$ at the interface of $HfO_2$–CdHgTe.

## 4. Conclusion

This paper studied the possibility of improvement of the electrophysical parameters of the interface of PE-ALD $HfO_2$–CdHgTe using low-temperature treatments of the CdHgTe surface applied directly in the chamber of atomic layer deposition of a dielectric. The following coatings were formed on a chemically cleaned epitaxial film of $Cd_{0.22}Hg_{0.78}Te$: native oxide with thickness of $\sim 1$ and $\sim 2$ nm, aluminum nitride with thickness of $\sim 2$ nm, aluminum oxide with thickness of $\sim 4$ nm. It was found as a result of the chemical analysis of these coatings by the XPS method that the use of trimethylaluminium in combination with a remote plasma ignited in a mixture of nitrogen and

Parameters of the interface PE-ALD $HfO_2-CdHgTe$ calculated from the capacitance–voltage curves of the MIS structures

| Pretreatment surface of CdHgTe | $N_t$, $10^{11}$ $cm^{-2} \cdot V^{-1}$ | $N_{fix}$, $10^{12}$ $cm^{-2}$ | $N_D$, $10^{15}$ $cm^{-3}$ |
|---|---|---|---|
| Without treatment | 3.0 | −1.2 | 2.8 |
| Cleaning in $NH_4OH$ | 3.2 | −1.6 | 2.2 |
| PE-ALD AlN | 2.9 | −1.1 | 2.1 |
| PE-ALD $Al_2O_x$ | 1.0 | −1.5 | 1.2 |
| Oxidation in the remote oxygen plasma during 1 min | 4.4 | 0.3 | 4.9 |
| Oxidation in the remote oxygen plasma during 10 min | 9.6 | 1.9 | 3.8 |

oxygen (1 : 1) is accompanied by oxidation of the CdHgTe surface and does not results in the formation of Al−N bonds in the formed aluminum oxide film. At the same time, a high content of aluminum oxide and hydroxide is observed in aluminum nitride films deposited using an atmosphere of pure nitrogen. Additional studies are needed to clarify whether they are formed during the growth of the film or are the result of the transfer of samples to a chemical analysis chamber through a laboratory atmosphere.

MIS structures with CdHgTe native oxide have a positive built-in charge, the density of which increases with the thickness of the oxide, while other samples are characterized by a negative built-in dielectric charge with a density of $\sim 1 \cdot 10^{12}\,cm^{-2}$. The density of slow trap states near the dielectric–semiconductor interface, which result in the hysteresis of the C−V curve due to capturing charge carriers, is significantly determined by the intermediate layer. For instance, the lowest density which is several times lower than the density of the reference sample is achieved in a structure with $Al_2O_x$, and the highest density is achieved in structures with the CdHgTe native oxide. It was also found that the use of treatments followed by deposition of hafnium oxide results in an increase of the concentration of donor centers in the area of the space charge region of the CdHgTe. The concentration closest to the growth data is found in MIS structures with an intermediate layer of $Al_2O_x$.

With further development and optimization, the proposed method of application of treatments immediately before dielectric deposition may turn out to be an effective method of passivation of the CdHgTe surface, which will improve the characteristics of both produced devices (IR photodetectors) and those under development (THz detectors and emitters).

## Funding

The study was supported financially by a grant from the Russian Science Foundation (project No. 21-72-10134).

## Conflict of interest

The authors declare that they have no conflict of interest.

## References

[1] A. Rogalski. *Infrared detectors*, 2nd Edition, CRC Press, Taylor & Francis Group, New York (2011).
[2] V.Y. Aleshkin, A.A. Dubinov, V.V. Rumyantsev, M.A. Fadeev, O.L. Domnina, N.N. Mikhailov, S.A. Dvoretsky, F. Teppe, V.I. Gavrilenko, S.V. Morozov. J. Phys. Condens. Matter, **30**, 495301 (2018).
[3] V.M. Bazovkin, V.S. Varavin, V.V. Vasil'ev, A.V. Glukhov, D.V. Gorshkov, S.A. Dvoretsky, A.P. Kovchavtsev, Yu.S. Makarov, D.V. Marin, I.V. Mzhelsky, V.G. Polovinkin, V.G. Remesnik, I.V. Sabinina, Yu.G. Sidorov, G.Yu. Sidorov, A.S. Stroganov, A.V. Tsarenko, M.V. Yakushev, A.V. Latyshev. J. Commun. Technol. Electron., **64**, 1011 (2019).
[4] W. Hu, Z. Ye, L. Liao, H. Chen, L. Chen, R. Ding, L. He, X. Chen, W. Lu. Optics Lett., **39**, 5184 (2014).
[5] S. Ruffenach, A. Kadykov, V.V. Rumyantsev, J. Torres, D. Coquillat, D. But, S.S. Krishtopenko, C. Consejo, W. Knap, S. Winnerl, M. Helm, M.A. Fadeev, N.N. Mikhailov, S.A. Dvoretskii, V.I. Gavrilenko, S.V. Morozov, F. Teppe. APL Mater., **5**, 035503 (2017).
[6] A.A. Dubinov, V.Ya. Aleshkin, V.I. Gavrilenko, V.V. Rumyantsev, N.N. Mikhailov, S.A. Dvoretsky, V.V. Utochkin, S.V. Morozov. Kvant. elektron., **51** (2), 158 (2021). (in Russian).
[7] A.V. Galeeva, A.I. Artamkin, A.S. Kazakov, S.N. Danilov, S.A. Dvoretskiy, N.N. Mikhailov, L.I. Ryabova, D.R. Khokhlov. Beilstein J. Nanotechnol., **9**, 1035 (2018).
[8] C. Ailiang, S. Changhong, W. Fang, Ye Zhenhua. Infr. Phys. Technol., **114**, 103667 (2021).
[9] V.S. Meena, M.S. Mehata. Thin Solid Films, **731**, 138751 (2021).
[10] V. Kumar, R. Pal, P.K. Chaudhury, B.L. Sharma, V. Gopal. J. Electron. Mater., **34**, 1225 (2005).
[11] Xi Wang, Kai He, Xing Chen, Yang Li, Chun Lin, Qinyao Zhang, Zhenhua Ye, Liwei Xin, Guilong Gao, Xin Yan, Gang Wang, Yiheng Liu, Tao Wang, Jinshou Tian. AIP Advances, **10**, 105102 (2020).
[12] D.V. Gorshkov, E.R. Zakirov, G.Yu. Sidorov, I.V. Sabinina, A.K. Gutakovsky, V.I. Vdovin. Izv. vuzov. Fizika, **66** (6), 111 (2023). (in Russian).
[13] E.R. Zakirov, V.G. Kesler, G.Yu. Sidorov, A.P. Kovchavtsev. Semicond. Sci. Technol., **35** (2), 025019 (2020).
[14] E.R. Zakirov, V.G. Kesler, G.Yu. Sidorov, V.A. Golyashov, O.E. Tereshchenko, D.V. Marin, M.V. Yakushev. Journal of Structural Chemistry, **64** (3), 519 (2023).
[15] M.P. Seah, S.J. Spencer. Surf. Interface Anal., **35** (6), 515 (2003).
[16] Roy Winter, Jaesoo Ahn, Paul C. McIntyre, Moshe Eizenberg. J. Vac. Sci. Technol. B, **31** (3), 030604 (2013).
[17] M. Alevli, C. Ozgit, I. Donmez, N. Biyikli. J. Cryst. Growth, **335** (1), 51 (2011).
[18] S. Ilhom, A. Mohammad, D. Shukla, J. Grasso, B.G. Willis, A.K. Okyay, N. Biyikli. RSC Advances, **10**, 27357 (2020).
[19] H. Fukumizu, M. Sekine, M. Hori, P.C. McIntyre. Jpn. J. Appl. Phys., **59**, 016504 (2020).

[20] E.R. Zakirov, V.G. Kesler, G.Y. Sidorov. 2023 IEEE XVI Int. *Sci. and Techn. Conf. Actual Problems of Electronic Instrument Engineering* (*APEIE*) (Novosibirsk, Russian Federation, 2023) p. 30.
DOI: 10.1109/APEIE59731.2023.10347577
[21] A.V. Voitsekhovskii, S.N. Nesmelov, S.M. Dzyadukh, Russ. Phys. J. **58**, 540 (2015).
[22] S.M. Sze. *Physics of Semiconductor Devices* (Wiley, Hoboken, NJ, 2006).

*Translated by A.Akhtyamov*